JPET Fast Forward. Published on July 27, 2006 as DOI: 10.1124/jpet.106.108316




# Pharmacological Characterization of Novel CGRP Receptor Peptide Antagonists that are Selective for Human CGRP Receptors

Christopher K. Taylor, D. David Smith, Martin Hulce and Peter W. Abel

Departments of Pharmacology (C.K.T., P.W.A.) and Biomedical Sciences (D.D.S.), School of Medicine and Department of Chemistry (M.H.), College of Arts and Sciences, Creighton University, 2500 California Plaza, Omaha, Nebraska. 68178 USA.

a) Running Title: CGRP receptor antagonists selective for human CGRP receptors

b) Corresponding Author:

Peter W. Abel, Ph.D.

Creighton University School of Medicine

Department of Pharmacology

2500 California Plaza

Omaha, NE 68178

Telephone: (402) 280-3187

Fax: (402) 280-2142

e-mail: pabel@creighton.edu

c) Number of text pages: 37

Number of tables: 2

Number of figures: 4

Number of references: 21

Number of words in abstract: 249

Number of words in introduction: 517

Number of words in discussion: 1567

d) Nonstandard abbreviations: CGRP, α-calcitonin gene-related peptide; CL, calcitonin receptor-like receptor; RAMP1, receptor activity-modifying protein 1; $CGRP_{(8-37)}$, human α-calcitonin gene-related $peptide_{(8-37)}$; bzl-$CGRP_{(8-37)}$, [N-α-benzoyl]human α-$CGRP_{(8-37)}$; bzl-bn-$CGRP_{(8-37)}$, [N-α-benzoyl-$His^{10}$-benzyl]human α-$CGRP_{(8-37)}$; $K_B$ and $pA_2$, equilibrium dissociation constant; Boc, *N-α-tert*-butyloxycarbonyl; MBHA, *para*-

methylbenzhydrylamine; TFA, trifluoroacetic acid; RP-HPLC, reversed phase-high performance liquid chromatography; ESI-MS, electrospray-ionization mass spectrometry; cAMP, 3',5' cyclic adenosine monophosphate.

e) Recommended section assignment: Cardiovascular

**Abstract**

Human α-calcitonin gene-related peptide (CGRP) is a 37-residue neuropeptide that produces a variety of cardiovascular and other effects via activation of specific CGRP receptors that produce 3',5' cyclic adenosine monophosphate (cAMP). Functional CGRP receptors are a heterodimeric complex comprised of the heptahelical calcitonin receptor-like receptor and the single transmembrane receptor activity-modifying protein 1. Based on the known structures of the antagonist $CGRP_{(8-37)}$ and the human CGRP receptor, we designed novel CGRP receptor peptide antagonists with modifications to promote high affinity and selectivity for human CGRP receptors. Antagonist affinity ($K_B$) at CGRP receptors was determined using the mouse thoracic aorta and human SK-N-MC cells. In aorta, $CGRP_{(8-37)}$, bzl-$CGRP_{(8-37)}$ and bzl-bn-$CGRP_{(8-37)}$ caused rightward shifts in the concentration-response relaxation curve for CGRP with $K_B$ values of 1000, 88 and 50 nM, respectively. In human SK-N-MC cells $CGRP_{(8-37)}$, bzl-$CGRP_{(8-37)}$ and bzl-bn-$CGRP_{(8-37)}$ caused rightward shifts in the concentration-response curve for CGRP stimulated cAMP production with $K_B$ values of 797, 15 and 0.63 nM, respectively. Thus, $CGRP_{(8-37)}$ had the same affinity for human and mouse CGRP receptors while bzl-$CGRP_{(8-37)}$ and bzl-bn-$CGRP_{(8-37)}$ displayed 6-fold and 80-fold higher affinity, respectively, for human CGRP receptors. In addition, the selectivity of the antagonists for human CGRP receptors was highly correlated with the antagonist hydrophobicity index. These relatively high affinity, species selective peptide antagonists provide novel tools to differentiate structural and functional features that are unique to the human CGRP receptor. Thus, these analogues may be useful compounds for development of drugs to treat migraine headache and other cardiovascular diseases.

## Introduction

Calcitonin gene-related peptide (CGRP) is an endogenous 37-amino acid neuropeptide that produces its effects by activation of specific G protein-coupled receptors located at the cell surface. Functional CGRP receptors are a 1:1 heterodimeric protein complex comprised of the heptahelical calcitonin receptor-like receptor (CL) and an accessory protein termed receptor activity-modifying protein 1 (RAMP1) (McLatchie et al., 1998; Poyner et al., 2002). Co-expression of CL with RAMP1 is necessary to produce a functional CGRP receptor. CGRP receptors in most tissues and cell lines are coupled to the $G_S$ family of heterotrimeric G-proteins and to an increase in 3',5' cyclic adenosine monophosphate (cAMP) (Aiyar et al., 1999). In humans, excessive CGRP-mediated cerebrovascular dilation plays an important role in the pathophysiology of headache. Currently BIBN4096BS, a non-peptide CGRP receptor antagonist, is in clinical trials for the treatment of migraine headache (Doods et al., 2000).

The exact mechanism of how the CGRP receptor, composed of CL and RAMP1, binds CGRP and/or CGRP antagonists is unknown. It has been proposed that the extracellular domain of RAMP1 may participate directly in ligand binding or act indirectly to modulate the ligand binding conformation of CL (Hilairet et al., 2001). The affinity of non-peptide antagonists for CGRP receptors has been shown to be modulated by amino acid residues residing in the extracellular domain of RAMP1 which provides evidence that RAMP1 directly participates in antagonist binding (Mallee et al., 2002). Based on the amino acid composition and analysis of hydropathy plots of CL and RAMP1, we hypothesized that RAMP1 forms a hydrophobic binding pocket with CL. The mouse CL shares 90% amino acid residues with human CL (Miyauchi et al., 2002).

In contrast, mouse RAMP1 shares only 71% amino acid residues with human RAMP1 (Husmann et al., 2000) and most of the amino acid sequence dissimilarity resides in the extracellular domain of RAMP1. Furthermore, hydropathy plots of human and mouse RAMP1 are markedly different in the N-terminus of the extracellular domain and indicate that human RAMP1 is more hydrophobic. Based on amino acid hydrophobicity differences between human and mouse RAMP1, we designed and synthesized a novel competitive antagonist, N-α-benzoyl-[His(4-benzyl)$^{10}$]-hα-CGRP$_{(8-37)}$ (bzl-bn-CGRP$_{(8-37)}$). This antagonist was designed to favor interaction with human RAMP1 by hydrophobic modifications we predicted would confer species selectivity due to the more hydrophobic amino acid composition of human RAMP1.

Knockout mice and other mouse assays are gaining increasing importance as model systems to understand human cardiovascular functions. Therefore, we characterized the standard CGRP receptor antagonist CGRP$_{(8-37)}$, our previously reported high affinity competitive antagonist N-α-benzoyl-hα-CGRP$_{(8-37)}$ (bzl-CGRP$_{(8-37)}$) (Smith et al., 2003) and the new antagonist, bzl-bn-CGRP$_{(8-37)}$ at mouse CGRP receptors, using the mouse thoracic aorta, and at human CGRP receptors, using the human SK-N-MC cell line. Comparison of antagonist affinities showed that bzl-bn-CGRP$_{(8-37)}$ is a relatively high affinity competitive antagonist that is selective for human compared to mouse CGRP receptors. Correlations between antagonist affinities and the hydrophobicity index of these antagonists suggest that hydrophobicity of the antagonist is a key factor in human CGRP receptor selectivity. This study may facilitate the design of high affinity human selective CGRP receptor antagonists for treatment of cardiovascular and other diseases.

## Methods

**Drugs and chemicals.** $CGRP_{(8-37)}$, bzl-$CGRP_{(8-37)}$ and bzl-bn-$CGRP_{(8-37)}$ were synthesized as described below. CGRP, *N*-*α*-*tert*-butyloxycarbonyl (Boc) amino acids and *para*-methylbenzhydrylamine (MBHA) resin were purchased from Bachem Inc. (Torrance, CA). Norepinephrine bitartrate, isoproterenol bitartrate, forskolin and Sigmacote were purchased from Sigma-Aldrich (St. Louis, MO). Isobutylmethylxanthine was purchased from EMD Biosciences Inc. (San Diego, CA). Trifluoroacetic acid (TFA), other solvents and chemicals were purchased from Fisher Scientific (Pittsburgh, PA). Dubelco's modified Eagle's medium, fetal bovine serum, and antibiotic/antimycotic (containing 10,000 units/mL penicillin G, 10,000 µg/mL streptomycin sulfate and 25 µg/mL amphotericin B) were purchased from Invitrogen (Carlsbad, CA).

**Hydropathy analysis of human and mouse CL and RAMP1 proteins.** Hydropathy analysis of human and mouse CL and RAMP1 proteins was carried out according to the Kyte-Doolittle method (window length 19) by use of the Protein Identification and Analysis Tool, ProtScale, on the Expert Protein Analysis System (ExPASy) server (Gasteiger et al., 2003; Gasteiger et al., 2005). The calculated hydropathy score was used to determine the hydrophobicity of the RAMP1 proteins.

**Solid phase peptide synthesis, purification and characterization.** Peptides were synthesized by Merrifield's solid-phase methods employing *in situ* neutralization (Schnolzer et al., 1992) using Boc amino acids and MBHA resin. Details of peptide synthesis are provided in previous publications (Smith et al., 2003; Taylor et al., 2005). Peptides were purified to >98% by semi-preparative reversed-phase high performance liquid chromatography (RP-HPLC) on a Vydac 218TP510 $C_{18}$ column (1 cm x 25 cm)

from the Separations Group (Hesperia, CA). Analytical RP-HPLC was performed on a Vydac 218TP5415 $C_{18}$ column (0.46 cm x 15 cm). All peptides were structurally characterized by amino acid analysis and electrospray-ionization mass spectrometry (ESI-MS). Amino acid analyses were performed using an AccQTag system from Waters (Milford, MA) after samples were hydrolyzed in constant boiling 6 M HCl at 110 °C for 24 h. ESI-MS was performed on an API150EX instrument from PE-SCIEX (Foster City, CA).

$CGRP_{(8-37)}$ and bzl-$CGRP_{(8-37)}$ were synthesized and purified as previously described (Smith et al., 2003; Taylor et al., 2005). Synthesis of bzl-bn-$CGRP_{(8-37)}$ was carried out manually in a 30 mL glass reaction vessel on a 0.5 mmol scale. A portion of the fully protected peptide-resin (100 mg, 0.02 mmol) was benzylated, then benzoylated as previously described (Smith et al., 2003). The peptide was cleaved from the resin and the crude product was loaded onto a $C_{18}$ RP-HPLC column. The product was eluted and fractions containing the desired product were identified by analytical RP-HPLC, pooled and lyophilized to yield 4 mg (6%) as a fluffy white powder.

**Hydrophobicity index.** Quantitation of the hydrophobicity of each peptide was determined by the retention time of the peptide on an RP-HPLC column. The hydrophobicity index was measured using three different RP-HPLC columns, column 1 was a Vydac $C_{18}$ monomeric 238TP54 column (250 x 4.6 mm), column 2 was a Waters Symmetry $C_{18}$ 300 Å column (250 x 4.6 mm) and column 3 was a Kromasil $C_8$ column (250 x 4.6 mm). Peptides were isocratically eluted with 0.1% TFA in water/acetonitrile 69/31 (v/v) at a flow rate of 1 mL/min and detected at 214 nm. The hydrophobicity index was calculated for each peptide by the formula, hydrophobicity index = $(t_R - t_0) / t_0$,

where $t_R$ is the retention time of the peptide and $t_0$ is the retention time of unretained material.

**Measurement of thoracic aorta relaxation.** Male albino mice (CF1, 25-35g) were obtained from Charles River Laboratories (Wilmington, MA). Mice were euthanized using $CO_2$ and thoracic aortas were removed and placed in Krebs' solution (composition in mM: NaCl, 118; KCl, 4.7; $CaCl_2$, 2.5; $KH_2PO_4$, 1.2; $MgSO_4$, 1.2; $NaHCO_3$, 25; dextrose, 11.1; $Na_2Ca$ EDTA, 0.029; pH 7.4). The aorta was cleaned of adhering connective tissue, endothelium was removed by gentle rubbing of the vessel lumen and the aorta cut into 3-mm long ring segments. Ring segments were mounted between two stainless steel pins passed through the vessel lumen and placed in water-jacketed organ baths maintained at 37 °C which contained Krebs' solution gassed with 95% $O_2$/5% $CO_2$, pH 7.4. The glass organ baths were coated with Sigmacote to reduce the binding of peptides to the glass surfaces. One pin was attached to a Grass FT.03 isometric force transducer (Grass Instruments, Quincy, MA) for measurement of isometric tension while the other pin was held in a fixed position. Ring segments were equilibrated in Krebs' solution for 30 min at a resting tension of 300 mg, contracted with 60 mM KCl followed by KCl washout and a 30 min equilibration period. Ring segments were contracted a second time with 60 mM KCl and the absence of endothelium was assessed by lack of relaxation caused by 1 μM of the endothelium-dependent vasodilator acetylcholine. The ring segments were then thoroughly washed for 30 min with Krebs' solution.

CGRP analogues were tested for both agonist and antagonist activity. For agonist studies analogues were tested for their ability to change resting tone and to alter the tone

JPET Fast Forward. Published on July 27, 2006 as DOI: 10.1124/jpet.106.108316
This article has not been copyedited and formatted. The final version may differ from this version.



of aortic ring segments precontracted to a stable level of tone with 1 μM norepinephrine. For antagonist studies, aortic ring segments were contracted with 1 μM norepinephrine for 20 min to obtain a stable amount of contractile tone (423 ± 44 mg) and cumulative CGRP concentration-response relaxation curves were obtained. Ring segments were then incubated with $CGRP_{(8-37)}$, bzl-$CGRP_{(8-37)}$ or bzl-bn-$CGRP_{(8-37)}$ for 60 min, contracted with 1 μM norepinephrine and cumulative CGRP concentration-response relaxation curves were repeated. Thus, two relaxant concentration-response curves to CGRP were generated in each aortic ring, a CGRP control and CGRP in the presence of antagonist. The spontaneous decline in tension of aortic rings contracted with norepinephrine averaged 12 ± 3 % during the time course of CGRP relaxation experiments. To test for non-specific effects and receptor specificity of the antagonism, the same analogue treatment protocol described above was used except that isoproterenol, rather than CGRP, was employed as the relaxant agonist.

**Measurement of cAMP production.** SK-N-MC cells were seeded and grown to confluence in CellStar 24-well plates (Greiner Bio-One Inc., Longwood, FL) in Dubelco's Modified Eagles Medium (DMEM) supplemented with fetal bovine serum (10%), penicillin G (100 units/mL), streptomycin (100 μg/mL) and amphotericin B (0.25 μg/mL). DMEM culture media was removed and the cells washed 3 times with 200 μL of HEPES-Krebs' buffer (composition in mM: NaCl, 118; KCl, 4.7; $CaCl_2$, 2.5; $KH_2PO_4$, 1.3; $MgSO_4$, 1.2; $NaHCO_3$, 15; Dextrose, 11.1; HEPES acid, 12.4; HEPES-Na, 7.5; isobutylmethylxanthine, 0.5; pH 7.4). HEPES-Krebs' buffer (900 μL) was added to each well and the plates incubated for 10 min in a humidified atmosphere at 37 °C. CGRP, forskolin or isoproterenol was added to various wells and the plates incubated for 30 min

in a humidified atmosphere (95% air/5% $CO_2$) at 37 °C. The cells were then lysed by addition of 150 μL of 95% ethanol and the cell lysate was dried in an oven at 40 ° C. cAMP production was measured by radioassay according to the manufacturer's protocol (Diagnostics Products Corporation, Los Angeles, CA). Radioactivity was measured using a Beckman LS 6000IS Scintillation counter.

To test for agonist activity, the CGRP analogues alone were added to wells for 15 min. To generate CGRP concentration-response curves, different concentrations of CGRP were added to various wells. To test for antagonist activity other wells were incubated with a single concentration of $CGRP_{(8-37)}$, bzl-$CGRP_{(8-37)}$ or bzl-bn-$CGRP_{(8-37)}$ for 15 min, followed by addition of various concentrations of CGRP. After drug treatments the plates were incubated for 30 min in a humidified atmosphere at 37 °C and cAMP production measured. To test for non-specific effects and receptor specificity of the antagonism, the same treatment protocol described above was used except that either 0.3 μM forskolin or 3 nM isoproterenol, rather than CGRP, was used to stimulate cAMP production.

**Calculation of equilibrium dissociation constants and data analysis.** $pA_2$ values for $CGRP_{(8-37)}$, bzl-$CGRP_{(8-37)}$ and bzl-bn-$CGRP_{(8-37)}$ were determined as described by Arunlakshana and Schild (1959). In mouse aorta, three adjacent ring segments from each animal were treated with different concentrations of $CGRP_{(8-37)}$, bzl-$CGRP_{(8-37)}$ or bzl-bn-$CGRP_{(8-37)}$. In separate experiments using different groups of SK-N-MC cells, cells were treated with different concentrations of bzl-bn-$CGRP_{(8-37)}$. For each concentration of antagonist used, dose ratios were calculated as the $EC_{50}$ value of CGRP in the presence of antagonist divided by the $EC_{50}$ value of CGRP in the absence of

antagonist. $EC_{50}$ values were calculated using all points on the relaxation or cAMP production concentration-response curves using least sum of squares nonlinear regression curve fitting with Graphpad Prism 4.0 (San Diego, CA). Schild plots were constructed by plotting log dose ratio − 1 *versus* the log of the antagonist concentration. Linear regression of the plotted points was used to determine the *x*-intercept ($pA_2$). In other experiments $K_B$ values for antagonists were determined using a single concentration of antagonist from the following equation: log $K_B$ = log [antagonist] – log (dose ratio – 1). Individual $pA_2$ or $pK_B$ values were averaged and compared statistically as log values. For convenience, they are listed in the text and table as arithmetic mean values ± S.E.M. after conversion to their antilogs.

Differences in maximal force generated by norepinephrine, isoproterenol $EC_{50}$ values, basal, forskolin-stimulated and isoproterenol-stimulated cAMP production, in the absence and presence of bzl-bn-$CGRP_{(8-37)}$, were compared using a Student's *t*-test with a $p < 0.05$ level of probability accepted as a significant difference. Differences in antagonist affinity values (mean $K_B$ values and mean $pA_2$ values) within an assay and between assays were determined using analysis of variance followed by Bonferroni post test with a $p < 0.05$ level of probability accepted as a significant difference. The slopes of the Schild regressions were analyzed for departure from linearity using analysis of variance followed by a Dunnett's post test with a $p < 0.05$ level of probability accepted as a significant difference from a slope of 1.

Correlation plots were constructed to compare antagonist affinities ($pK_B$) in the mouse aorta, antagonist affinities ($pK_B$) in human SK-N-MC cells and antagonist hydrophobicity. These data are expressed as the mean of individual log values or their

reciprocals ± 95% confidence interval. The antagonist hydrophobicity index was determined using three different RP-HPLC systems.

## Results

**Hydropathy analysis of human and mouse CL and RAMP1 proteins.** Using ProtScale on the ExPASy server we constructed hydropathy plots to compare hydrophobicity between human and mouse CL and between human and mouse RAMP1. The human and mouse CL share high amino acid sequence identity (90%) and as illustrated by the hydropathy plot, Fig. 1A, are nearly identical in their hydrophobicity. In contrast, human and mouse RAMP1 share only 71% amino acid sequence identity and most of the non-conserved amino acids reside in the extracellular domain. The hydrophobicity of the transmembrane and intracellular domains of RAMP1 are nearly identical while the extracellular domains are markedly different as illustrated by the hydropathy plot, Fig. 1B. Analysis of the hydrophobicity of human and mouse RAMP1 revealed that the extracellular domain of human RAMP1 is 62% more hydrophobic than mouse RAMP1. Furthermore, most of the increased hydrophobicity occurred in the extreme N-terminus of the extracellular domain of human RAMP1.

**Peptide synthesis and characterization.** Novel analogues of the antagonist $CGRP_{(8-37)}$ containing modifications to the N-terminus and the imidazole side chain of histidine at position 10 were synthesized manually by solid-phase methods employing *in situ* neutralization using Boc-amino acids. (Schnolzer et al., 1992; Taylor et al., 2005) The peptides were purified by semi-preparative RP-HPLC. Peptide purity was > 98% by analytical RP-HPLC under isocratic elution conditions using three different RP-HPLC columns. The purified products had the correct masses as determined by ESI-MS and satisfactory amino acid composition (Table 1). As predicted, low recovery of valine was found in the composition of bzl-CGRP(8-37) and bzl-bn-CGRP(8-37) which is consistent

JPET Fast Forward. Published on July 27, 2006 as DOI: 10.1124/jpet.106.108316
This article has not been copyedited and formatted. The final version may differ from this version.



with benzoylation of the N-terminal valine residue. No histidyl residue was found in the amino acid composition of bzl-bn-$CGRP_{(8-37)}$ which is consistent with irreversible benzylation of the histidyl residue at position 10 in this analogue.

The hydrophobicity of the peptide analogues was measured by RP-HPLC using three different RP-HPLC columns. The hydrophobicity index of $CGRP_{(8-37)}$, bzl-$CGRP_{(8-37)}$ and bzl-bn-$CGRP_{(8-37)}$ using column 1 (Vydac) was 0.1, 0.7 and 2.1, respectively; column 2 (Waters Symmetry) was 0.1, 0.9 and 3.1, respectively; column 3 (Kromasil) was 0.5, 1.0 and 2.7, respectively. The rank order of hydrophobicity was bzl-bn-$CGRP_{(8-37)}$ > bzl-$CGRP_{(8-37)}$ > $CGRP_{(8-37)}$ and was the same among all RP-HPLC columns used.

**Evaluation of agonist activity and non-specific effects of bzl-bn-$CGRP_{(8-37)}$ in mouse aorta.** Using mouse aorta we tested the novel CGRP receptor antagonist, bzl-bn-$CGRP_{(8-37)}$, for agonist activity to cause relaxation by precontracting aorta with 1 μM norepinephrine and determining the effects of addition of 1 μM of this antagonist. bzl-bn-$CGRP_{(8-37)}$ (1 μM) had no significant effect on norepinephrine induced tone of aorta (data not shown). In addition, 1 μM bzl-bn-$CGRP_{(8-37)}$ had no effect on the resting level of tone in this tissue (data not shown). We also determined if bzl-bn-$CGRP_{(8-37)}$ had non-specific effects to interfere with norepinephrine-mediated contraction by measuring the amount of tension produced by 1 μM norepinephrine in the absence and presence of this antagonist. There was no significant difference in the amount of norepinephrine-induced contractile tone in the absence (185 ± 15 mg, $n$ = 12) compared to the presence (195 ± 17 mg, $n$ = 12) of 1 μM of bzl-bn-$CGRP_{(8-37)}$.

**Affinity of $CGRP_{(8-37)}$, bzl-$CGRP_{(8-37)}$ and bzl-bn-$CGRP_{(8-37)}$ for CGRP receptors in mouse aorta.** CGRP produced concentration-dependent relaxation to the

JPET Fast Forward. Published on July 27, 2006 as DOI: 10.1124/jpet.106.108316
This article has not been copyedited and formatted. The final version may differ from this version.



baseline level of tone with an $EC_{50}$ value of 10 ± 1.0 nM (Fig. 2A). In the presence of $CGRP_{(8-37)}$, bzl-$CGRP_{(8-37)}$ and bzl-bn-$CGRP_{(8-37)}$ the CGRP concentration-response curves were shifted to the right in a parallel manner consistent with competitive antagonism (data not shown). $EC_{50}$ values for CGRP in the presence of $CGRP_{(8-37)}$ (10 μM), bzl-$CGRP_{(8-37)}$ (3 μM) and bzl-bn-$CGRP_{(8-37)}$ (1.5 μM) were 158 ± 52, 1945 ± 645 and 530 ± 126 nM, respectively. Using these data the affinities ($K_B$ values) of the antagonists were calculated and are listed in Table 2. The rank order of antagonist affinity was bzl-bn-$CGRP_{(8-37)}$ = bzl-$CGRP_{(8-37)}$ > $CGRP_{(8-37)}$.

The affinity of bzl-bn-$CGRP_{(8-37)}$, for CGRP receptors mediating relaxation of mouse aorta, was further evaluated by generating concentration-response relaxation curves for CGRP in the absence and presence of various concentrations of bzl-bn-$CGRP_{(8-37)}$. As shown in Fig. 2A, bzl-bn-$CGRP_{(8-37)}$ inhibited CGRP-induced relaxation and caused concentration-dependent rightward shifts in the CGRP concentration-response curve. These data were used to construct Schild plots (Fig. 2C) from which the affinity ($pA_2$ value) for bzl-bn-$CGRP_{(8-37)}$ in inhibiting CGRP-induced relaxation was calculated. The mean $pA_2$ value for bzl-bn-$CGRP_{(8-37)}$ calculated from the Schild regressions was 7.3 with a mean slope of 1.3 ± 0.1.

**Specificity of bzl-bn$CGRP_{(8-37)}$ interaction with CGRP receptors in mouse aorta.** bzl-bn$CGRP_{(8-37)}$ was also evaluated for the specificity of its CGRP receptor antagonism effect. After precontraction of mouse aorta with 1 μM norepinephrine, isoproterenol concentration-response relaxation curves in the absence and presence of 1 μM of bzl-bn$CGRP_{(8-37)}$ were generated. There was no significant effect on maximal isoproterenol-mediated relaxation of the aorta in the absence (100 ± 1 %, *n* = 4)

compared to the presence (98 ± 3 %, *n* = 4) of bzl-bn-CGRP$_{(8-37)}$ or on isoproterenol $EC_{50}$ values in the absence (36 ± 12 μM, *n* = 4) compared to the presence (46 ± 5 μM, *n* = 4) of bzl-bn-CGRP$_{(8-37)}$. Thus, bzl-bn-CGRP$_{(8-37)}$ does not cause non-specific inhibition of aortic relaxation at this concentration.

**Evaluation of agonist activity, non-specific effects and receptor specificity of bzl-bn-CGRP$_{(8-37)}$ in human SK-N-MC cells.** Mean basal, forskolin-stimulated and isoproterenol-stimulated cAMP production in SK-N-MC cells in the absence and presence of 1 μM of bzl-bn-CGRP$_{(8-37)}$ is shown in Fig. 3. There was no significant effect of bzl-bn-CGRP$_{(8-37)}$ on the basal level of cAMP production or on forskolin-stimulated cAMP production. This indicates that bzl-bn-CGRP$_{(8-37)}$ lacks intrinsic agonist activity and does not cause non-specific inhibition of adenylyl cyclase at this concentration. In addition, there was no significant effect of bzl-bn-CGRP$_{(8-37)}$ on isoproterenol-stimulated cAMP production, indicating that 1 μM of this antagonist does not non-specifically inhibit G protein-coupled receptor-mediated cAMP production (Fig. 3).

**Affinity of CGRP$_{(8-37)}$, bzl-CGRP$_{(8-37)}$ and bzl-bn-CGRP$_{(8-37)}$ for CGRP receptors in human SK-N-MC cells.** CGRP produced concentration-dependent increases in cAMP production with an $EC_{50}$ value of 5.7 ± 0.5 nM (Fig. 2B). In the presence of CGRP$_{(8-37)}$, bzl-CGRP$_{(8-37)}$ and bzl-bn-CGRP$_{(8-37)}$ the CGRP concentration-response curves were shifted to the right in a parallel manner (data not shown). $EC_{50}$ values for CGRP in the presence of CGRP$_{(8-37)}$ (1 μM), bzl-CGRP$_{(8-37)}$ (0.025 μM) and bzl-bn-CGRP$_{(8-37)}$ (0.1 μM) were 31 ± 14, 20 ± 1 and 133 ± 29 nM, respectively. The $EC_{50}$ values from these concentration-response curves were used to calculate antagonist

JPET Fast Forward. Published on July 27, 2006 as DOI: 10.1124/jpet.106.108316
This article has not been copyedited and formatted. The final version may differ from this version.



affinity values which are listed in Table 2. The rank order of antagonist affinity was bzl-bn-$CGRP_{(8-37)}$ > bzl-$CGRP_{(8-37)}$ > $CGRP_{(8-37)}$.

The affinity of the most potent antagonist, bzl-bn-$CGRP_{(8-37)}$, for CGRP receptors mediating cAMP production in SK-N-MC cells was further evaluated by generating concentration-response curves for CGRP in the absence and presence of various concentrations of bzl-bn-$CGRP_{(8-37)}$. As shown in Fig. 2B, bzl-bn-$CGRP_{(8-37)}$ inhibited CGRP-induced cAMP production and caused concentration-dependent parallel rightward shifts in the CGRP concentration-response curve. These data were used to construct Schild plots (Fig. 2C) from which the affinity ($pA_2$ value) for bzl-bn-$CGRP_{(8-37)}$ in inhibiting CGRP-induced cAMP production was calculated. The mean $pA_2$ value for bzl-bn-$CGRP_{(8-37)}$ calculated from the Schild regression was 9.2 with a mean slope of 0.9 ± 0.1.

**Comparison of antagonist affinities in mouse aorta and human SK-N-MC cells and correlations with antagonist hydrophobicity.** Fig. 2C, shows mean Schild plots for the antagonist bzl-bn-$CGRP_{(8-37)}$ derived from the data shown in Fig. 2A and Fig. 2B. The mean $pA_2$ value was 80-fold lower (higher affinity) in human SK-N-MC cells (pA2 = 9.2) compared to the mean $pA_2$ value in the mouse aorta (pA2 = 7.3) (Fig. 2C).

We also compared antagonist affinity in inhibiting CGRP-induced relaxation in mouse aorta with antagonist affinity in inhibiting CGRP-induced cAMP production in human SK-N-MC cells for all antagonists using the data shown in Table 2. There was no difference in the affinity of $CGRP_{(8-37)}$ in the aorta compared to that in SK-N-MC cells (Table 2). In contrast, the affinity of bzl-bn-$CGRP_{(8-37)}$ was significantly higher in human

SK-N-MC cells compared to the mouse aorta (Table 2). Fig. 4A shows the correlation, for all antagonists, of their affinities in mouse aorta compared to their affinities in human SK-N-MC cells. The 95% confidence interval of mean $pK_B$ values for $CGRP_{(8-37)}$ included the line of identity while those values for bzl-$CGRP_{(8-37)}$ and bzl-bn-$CGRP_{(8-37)}$ did not. Thus, there was a statistically significant decrease in the slope of the regression line correlating affinities in human SK-N-MC cells and mouse aorta compared to the line of identity. These data show that bzl-$CGRP_{(8-37)}$ and bzl-bn-$CGRP_{(8-37)}$ both have a higher affinity for CGRP receptors in human SK-N-MC cells.

We also correlated antagonist affinity to inhibit CGRP-induced relaxation in mouse aorta and cAMP production in human SK-N-MC cells, with antagonist hydrophobicity (Fig. 4B). Increasing the hydrophobicity of the antagonists correlated with increases in the affinity of $CGRP_{(8-37)}$, bzl-$CGRP_{(8-37)}$ and bzl-bn-$CGRP_{(8-37)}$ in both the mouse aorta and human SK-N-MC cells. In human SK-N-MC cells, increasing antagonist hydrophobicity caused a linear, proportional increase in affinity. Thus, the linear regression line correlating these parameters in human SK-N-MC cells was not different from the line of identity. In contrast, in the mouse aorta the correlation between antagonist affinity and hydrophobicity was not proportional. Thus, in mouse aorta, there was a significant decrease in the slope of the regression line correlating affinity and hydrophobicity index compared to the line of identity.

**Discussion**

CGRP is a 37-residue neuropeptide that is widely distributed in the central and peripheral nervous systems. This peptide acts as a neurotransmitter and neuromodulator with important cardiovascular actions, which include regulation of peripheral vascular tone and force and rate of cardiac contraction. The actions of CGRP are mediated through CGRP receptors which are family B members of the G protein-coupled receptor superfamily. $CGRP_{(8-37)}$ is the primary pharmacological tool used to characterize CGRP receptors and the differential affinity of this antagonist in different tissues provides evidence for CGRP receptor heterogeneity. At this time, only one CGRP receptor, the CGRP-1 receptor, has been cloned. The CGRP-1 receptor consists of a heterodimer comprised of the calcitonin receptor-like receptor (CL) and receptor activity-modifying protein 1 (RAMP1) (McLatchie et al., 1998). To date, the International Union of Pharmacology and most other authorities recognize the CGRP-1 receptor subtype and a second heterogeneous population of CGRP receptors that may contain more than one pharmacologically distinct CGRP receptor subtype (Poyner et al., 2002).

The mouse is an important experimental animal model used to identify new agents for the treatment of cardiovascular disease. Effective use of the mouse as a model for human CGRP receptor-mediated effects requires an understanding of the pharmacological tools used to examine CGRP receptor-mediated responses and if these tools differentiate human CGRP receptors from CGRP receptors in other species. Despite the establishment of the mouse as a sensitive system to study the vasodilatory effects of CGRP (Pomerleau et al., 1997; Chan and Fiscus, 2001), there are no functional studies that quantify the affinity of the prototypical CGRP receptor antagonist $CGRP_{(8-37)}$ in

mouse blood vessels to identify the CGRP receptor type causing vascular relaxation. In our studies, we found that $CGRP_{(8-37)}$ had micromolar affinity ($pA_2$ = 6.4) in blocking CGRP induced relaxation of mouse aorta consistent with this response being mediated by CGRP-1 receptors. In addition, the affinity of $CGRP_{(8-37)}$ to inhibit relaxation was the same as its affinity to inhibit cAMP production in human SK-K-MC cells, which are routinely used as a model system to study CGRP-1 receptors. Thus, unlike blood vessels from some other species (Wisskirchen et al., 1999), we found that the mouse has typical CGRP-1 receptor mediated vascular relaxation as has been reported in isolated blood vessels from humans (Hasbak et al., 2003).

In addition to the prototypical CGRP receptor antagonist $CGRP_{(8-37)}$, we also quantitatively characterized a CGRP receptor antagonist, bzl-$CGRP_{(8-37)}$, previously identified by our laboratory (Smith et al., 2003), and a novel antagonist bzl-bn-$CGRP_{(8-37)}$. These three antagonists all acted in a competitive manner in blocking functional responses in mouse aorta and in human SK-N-MC cells and the rank order of affinity at CGRP receptors in both of these assay systems was bzl-bn-$CGRP_{(8-37)} \geq$ bzl-$CGRP_{(8-37)} >$ $CGRP_{(8-37)}$. Furthermore, the new antagonist, bzl-bn-$CGRP_{(8-37)}$, had no agonist activity or non-specific effects in both the aorta and SK-N-MC cell line at concentrations up to 1 μM. Correlations among the affinities of $CGRP_{(8-37)}$, bzl-$CGRP_{(8-37)}$ and bzl-bn-$CGRP_{(8-37)}$ in the mouse aorta compared to human SK-N-MC cells showed that $CGRP_{(8-37)}$ does not discriminate between mouse and human CGRP receptors. In contrast, bzl-$CGRP_{(8-37)}$ and bzl-bn-$CGRP_{(8-37)}$, have increased affinity for human CGRP receptors in SK-N-MC cells. We also measured antagonist hydrophobicity and found the same rank order of antagonist hydrophobicity of bzl-bn-$CGRP_{(8-37)}$ > bzl-$CGRP_{(8-37)}$ > $CGRP_{(8-37)}$, as for the

rank order of antagonist affinity. These correlations suggest that increasing the hydrophobic characteristics of these $CGRP_{(8-37)}$ based peptide antagonists provides progression toward human CGRP receptor selectivity.

We cannot rule out the possibility that tissue mediated peptide degradation, the binding of peptides to glass surfaces, or tissue barriers to diffusion of peptides into receptor compartments could all reduce the concentration of these antagonists at CGRP receptors leading to an underestimation of their affinities in functional assays using mouse aorta. However, our new antagonist peptides differ importantly from the standard antagonist $CGRP_{(8-37)}$ because they are N-terminally acylated. It is well established that derivatization of the N-terminus of peptides protects them from degradation by aminopeptidases (Drapeau et al., 1993) which suggest that metabolism of the antagonists is most likely minimal in our experiments. In addition, our organ chambers are coated with organosilanes which limits the binding of peptides and other agents to glass surfaces. This treatment would also reduce peptide loss in our experiments. We also found that the standard peptide antagonist, $CGRP_{(8-37)}$, had the same affinity in mouse aorta compared to SK-N-MC cells which indicates that, at least for this antagonist, diffusion barriers do not confound our affinity measurements in the mouse aorta. Although these experimental factors could contribute to differences in antagonist affinity among, we believe that these factors are not likely to explain the 80-fold difference in the affinity of bzl-bn-$CGRP_{(8-37)}$ between mouse aorta and SK-N-MC cells.

The N-terminus of family B G protein-coupled receptors plays a key role in ligand binding to receptors. For the CGRP receptor the extracellular domains of CL and RAMP1 are thought to form the binding site for peptide ligands (Fraser et al., 1999;

Koller et al., 2002), with RAMP1 being the most important component. The extracellular domain of RAMP1 is the least conserved region among species and amino acids 66 – 112 of this region are important for determining the affinity of the non-peptide antagonists BIBN4096BS and Compound 1 for CGRP receptors (Mallee et al., 2002). These non-peptide antagonists show selectivity for the human compared to the rodent CGRP receptor and a single amino acid at position 74 in the extracellular domain of RAMP1 has been reported to explain this species selectivity. The fact that our new peptide antagonist bzl-bn-CGRP$_{(8-37)}$, also showed relatively high affinity and human CGRP receptor selectivity suggests that the extracellular domain of RAMP1 may be necessary for CGRP receptor interaction with both peptide and non-peptide antagonists. In our studies, we found that bzl-CGRP$_{(8-37)}$ and bzl-bn-CGRP$_{(8-37)}$ have up to 80-fold higher affinity for the human compared to the mouse CGRP receptor. We propose that this species difference in affinity may be accounted for by sequence dissimilarity in the extracellular domain between human and mouse RAMP1. In fact, comparison of the extracellular domain amino acid composition between human and mouse RAMP1, using the Kyte-Doolittle hydrophobicity scale (Kyte and Doolittle, 1982), showed numerous amino acid differences resulting in an extracellular domain of human RAMP1 that is 62% more hydrophobic compared to mouse RAMP1. These findings indicate that the CGRP receptor binding pocket formed by the extracellular domains of human CL and RAMP1 may be more hydrophobic than the binding pocket formed between the extracellular domains of mouse CL and RAMP1.

Important information about ligand binding sites on the native CGRP receptor can be gained by comparing the interaction of peptide and non-peptide antagonists which can

be used to guide modeling of receptor-ligand interaction. Although there is a significant size difference between the low molecular weight non-peptide antagonists BIBN4096BS and Compound 1 compared to our new peptide antagonists, both interact with RAMP1 and their human selectivity is directed by RAMP1. While non-peptide antagonists require only a single amino acid residue on RAMP1 to confer human selectivity, peptide antagonists appear to require a wider amino acid region for this interaction. Hydropathy plots of human and mouse RAMP1 show that the region encompassing position 74, the amino acid responsible for human selectivity of non-peptide antagonists, is more hydrophobic in mouse RAMP1 (Fig. 1). This shows that human selective non-peptide antagonists have a greater affinity for the extracellular domain of human RAMP1 which is less hydrophobic than mouse RAMP1. Thus, for non-peptide antagonists decreasing hydrophobic interactions between ligand and receptor are correlated with human selectivity of these antagonists. Our new peptide antagonist bzl-bn-$CGRP_{(8-37)}$ was designed with hydrophobic modifications to the region of this peptide that is thought to interact with the hydrophobic extreme N-terminus of the extracellular domain of human RAMP1. Our correlations between antagonist affinities and their hydrophobicity indicate that increasing hydrophobicity of peptide antagonists is a key factor in human CGRP receptor selectivity. Based on a hydrophobic interaction between our new peptide antagonists and RAMP1 we predict they interact with the region of human RAMP1 that is more hydrophobic than the mouse, residues 55 to the N-terminus. Thus, peptide and non-peptide antagonists appear to interact in a different manner with RAMP1 and there may be a difference in the structural determinants within the CGRP receptor that contribute to their species selectivities. These human selective peptide antagonists

provide novel tools to study the integrative processes that cause functional responses in native cells, tissues and animals, the functionome.

In summary, we designed, synthesized and measured the affinity of $CGRP_{(8-37)}$, and the more hydrophobic antagonists bzl-$CGRP_{(8-37)}$ and bzl-bn-$CGRP_{(8-37)}$ at mouse and human CGRP receptors. We found that $CGRP_{(8-37)}$, does not discriminate between mouse and human CGRP receptors, while bzl-$CGRP_{(8-37)}$ possesses some preference for human CGRP receptors. In contrast, the most hydrophobic antagonist, bzl-bn-$CGRP_{(8-37)}$, possessed the highest affinity and greatest selectivity for human CGRP receptors. The modification of $CGRP_{(8-37)}$ with bulky hydrophobic groups resulting in relatively high affinity peptide antagonists at human receptors suggests that human CGRP receptor selectivity is directed by the extreme N-terminus of the extracellular domain of RAMP1 which participates as a unique entity for peptide antagonists forming a hydrophobic binding pocket with CL. We propose that the species selectivity of these peptide antagonists is due to increased hydrophobic ligand-receptor interactions. Thus, the N-terminus of the extracellular domain of human RAMP1 is a critical target to exploit for development of human selective CGRP receptor agents.

**Acknowledgements**

We thank Dr. Donald R. Babin for performing amino acid analysis and Dr. Charles Bockman for helpful comments.

## References

Aiyar N, Disa J, Stadel JM and Lysko PG (1999) Calcitonin gene-related peptide receptor independently stimulates 3',5'- cyclic adenosine monophosphate and Ca2+ signaling pathways. *Mol Cell Biochem* **197**:179-185.

Chan S and Fiscus R (2001) Vasorelaxant response to isoprenaline, nitric oxide donor, calcitonin gene-related peptide and vasoactive intestinal peptide in aortic rings of adult C57BL/6J mice. *Eur J Pharmacol* **431**:229-236.

Doods H, Hallermayer G, Wu D, Entzeroth M, Rudolf K, Engel W and Eberlein W (2000) Pharmacological profile of BIBN4096BS, the first selective small molecule CGRP antagonist. *Br J Pharmacol* **129**:420-423.

Drapeau G, Audet R, Levesque L, Godin D and Marceau F (1993) Development and in vivo evaluation of metabolically resistant antagonists of B1 receptors for kinins. *J Pharmacol Exp Ther* **266**:192-199.

Fraser NJ, Wise A, Brown J, McLatchie LM, Main MJ and Foord SM (1999) The amino terminus of receptor activity modifying proteins is a critical determinant of glycosylation state and ligand binding of calcitonin receptor-like receptor. *Mol Pharmacol* **55**:1054-1059.

Gasteiger E, Gattiker A, Hoogland C, Ivanyi I, Appel RD and Bairoch A (2003) ExPASy: The proteomics server for in-depth protein knowledge and analysis. *Nucleic Acids Res* **31**:3784-3788.

Gasteiger E, Hoogland C, Gattiker A, Duvaud S, Wilkins MR, Appel RD and Bairoch A (2005) Protein Identification and Analysis Tools on the ExPASy Server, in *The Proteomics Protocols Handbook* (Walker JM ed) pp 571-607, Humana Press, Totowa.

Hasbak P, Saetrum Opgaard O, Eskesen K, Schifter S, Arendrup H, Longmore J and Edvinsson L (2003) Investigation of CGRP receptors and peptide pharmacology in human coronary arteries. Characterization with a nonpeptide antagonist. *J Pharmacol Exp Ther* **304**:326-333.

Hilairet S, Foord SM, Marshall FH and Bouvier M (2001) Protein-protein interaction and not glycosylation determines the binding selectivity of heterodimers between the calcitonin receptor- like receptor and the receptor activity-modifying proteins. *J Biol Chem* **276**:29575-29581.

Husmann K, Sexton PM, Fischer JA and Born W (2000) Mouse receptor-activity-modifying proteins 1, -2 and -3: amino acid sequence, expression and function. *Mol Cell Endocrinol* **162**:35-43.

Koller D, Born W, Leuthauser K, Fluhmann B, McKinney RA, Fischer JA and Muff R (2002) The extreme N-terminus of the calcitonin-like receptor contributes to the selective interaction with adrenomedullin or calcitonin gene-related peptide. *FEBS Lett* **531**:464-468.

Kyte J and Doolittle RF (1982) A simple method for displaying the hydropathic character of a protein. *J Mol Biol* **157**:105-132.

Mallee JJ, Salvatore CA, LeBourdelles B, Oliver KR, Longmore J, Koblan KS and Kane SA (2002) Receptor activity-modifying protein 1 determines the species selectivity of non-peptide CGRP receptor antagonists. *J Biol Chem* **277**:14294-14298.

McLatchie LM, Fraser NJ, Main MJ, Wise A, Brown J, Thompson N, Solari R, Lee MG and Foord SM (1998) RAMPs regulate the transport and ligand specificity of the calcitonin- receptor-like receptor. *Nature* **393**:333-339.

Miyauchi K, Tadotsu N, Hayashi T, Ono Y, Tokoyoda K, Tsujikawa K and Yamamoto H (2002) Molecular cloning and characterization of mouse calcitonin gene-related peptide receptor. *Neuropeptides* **36**:22-33.

Pomerleau F, Fournier A and Cadieux A (1997) Mouse aorta: a preparation highly sensitive to the vasodilatory action of CGRP. *J Cardiovasc Pharmacol* **30**:343-351.

Poyner DR, Sexton PM, Marshall I, Smith DM, Quirion R, Born W, Muff R, Fischer JA and Foord SM (2002) International Union of Pharmacology. XXXII. The mammalian calcitonin gene-related peptides, adrenomedullin, amylin, and calcitonin receptors. *Pharmacol Rev* **54**:233-246.

Schnolzer M, Alewood P, Jones A, Alewood D and Kent SB (1992) In situ neutralization in Boc-chemistry solid phase peptide synthesis. Rapid, high yield assembly of difficult sequences. *Int J Pept Protein Res* **40**:180-193.

Smith DD, Saha S, Fang G, Schaffert C, Waugh DJ, Zeng W, Toth G, Hulce M and Abel PW (2003) Modifications to the N-terminus but not the C-terminus of calcitonin gene-related peptide(8-37) produce antagonists with increased affinity. *J Med Chem* **46**:2427-2435.

Taylor CK, Abel PW, Hulce M and Smith DD (2005) Solvent effects on coupling yields during rapid solid-phase synthesis of CGRP(8-37) employing in situ neutralization. *J Pept Res* **65**:84-89.

Wisskirchen FM, Gray DW and Marshall I (1999) Receptors mediating CGRP-induced relaxation in the rat isolated thoracic aorta and porcine isolated coronary artery differentiated by h(alpha) CGRP(8-37). *Br J Pharmacol* **128**:283-292.

**Footnotes**

This work was supported by an American Heart Association Pre-Doctoral Fellowship (C.K.T.) and NIH grant P20 RR16469.

**Legends for Figures**

**Fig. 1.** Hydropathy plot overlays of predicted human and mouse CL (**Panel A**) and RAMP1 (**Panel B**) amino acid sequences. The regions of the hydropathy plots on the left represent the extracellular N-terminus and the labeled segments on the right represent the transmembrane (TM) domains and intracellular C-terminus. The hydropathy plot of human and mouse CL are nearly identical while the hydropathy plot of human and mouse RAMP1 are markedly different, particularly at the end of the N-terminus of the extracellular domain. The region that is more hydrophobic in human RAMP1, where hydrophobic peptide antagonists are proposed to interact, is labeled Human > Mouse. The region more hydrophobic in the mouse and where non-peptide antagonists interact is labeled Mouse > Human, amino acids 66 – 112 and position 74. Hydropathy plots were drawn using the Kyte-Doolittle method by use of ProtScale on the ExPASy server. Positive numbers indicate calculated hydrophobic amino acid regions while negative numbers indicate calculated hydrophilic amino acid regions.

**Fig. 2 Panel A.** Effect of different concentrations of bzl-bn-$CGRP_{(8-37)}$ on concentration-response curves for CGRP-induced relaxation of mouse aorta. Concentration-response curves are plotted as percent relaxation to the baseline tone present before contraction with 1 μM norepinephrine. Points are the mean ± S.E.M. of responses of four to six individual thoracic aortas, each taken from different animals. **Panel B.** Effect of different concentrations of bzl-bn-$CGRP_{(8-37)}$ on concentration-response curves for CGRP-stimulated cAMP production in SK-N-MC cells. Concentration-response curves are plotted as percent of the maximal CGRP-stimulated cAMP production. Points are the

mean ± S.E.M. of responses from three individual experiments performed in duplicate, with each experiment using cells grown in different culture plates on different days. **Pnael C.** Mean Schild plots of data from Fig. 2 Panel A using mouse aorta and from Fig. 2 Panel B using human SK-N-MC cells. The affinity ($pA_2$) of bzl-bn-$CGRP_{(8-37)}$ for CGRP receptors in the mouse aorta and human SK-N-MC cells was calculated as the *x*-intercept of the Schild plot which was 7.3 and 9.2, respectively.

**Fig. 3.** Effect of bzl-bn-$CGRP_{(8-37)}$ on basal, forskolin-stimulated and isoproterenol-stimulated cAMP production in SK-N-MC cells. Cells were incubated with vehicle (basal), 300 nM forskolin or 3 nM isoproterenol, in the absence (open bars) or presence of 1 μM bzl-bn-$CGRP_{(8-37)}$ (solid bars), for 30 min at 37 °C and cAMP production measured. Bars are the mean ± S.E.M. generated from three to fourteen individual experiments performed in duplicate, with each experiment using cells grown in different culture plates on different days.

**Fig. 4. Panel A.** Correlation plot of antagonist affinity values ($pK_B$) determined from data for CGRP receptor-mediated responses in the mouse aorta (Table 2) and human SK-N-MC cells (Table 2). The dashed line is the line of identity while the solid line is the Deming regression of the affinity of the antagonists in mouse aorta versus human SK-N-MC cells. Data points are mean ± 95% confidence intervals. The slope and correlation coefficient ($r^2$) of the linear regression of the data points are indicated. Note that the points for bzl-$CGRP_{(8-37)}$ and bzl-bn-$CGRP_{(8-37)}$ deviate from the line of identity while the point for $CGRP_{(8-37)}$ does not. **Panel B.** Correlation plot of the affinity values (log

($1/pK_B$)) determined from data for CGRP receptor-mediated responses in the mouse aorta (data from Table 2) or human SK-N-MC cells (data from Table 2) and the hydrophobicity index of the antagonists (data listed in results section). The dashed line is the line of identity while the solid line is the Deming regression of the affinity of the antagonists in mouse aorta (solid symbols) or human SK-N-MC cells (open symbols) versus the hydrophobicity of the individual analogues. Data points are mean ± 95% confidence intervals. Note that in mouse aorta, the points for bzl-$CGRP_{(8-37)}$ and bzl-bn-$CGRP_{(8-37)}$ deviate form the line of identity while the points for these antagonists in human SK-N-MC cells do not.

**Table 1.** Amino acid composition of $CGRP_{(8-37)}$ and N-terminal and $His^{10}$ modified analogues.

| Analogue | Asp | Ser | Gly | His[a] | Arg | Thr | Ala | Pro | Val[b] | Lys | Leu | Phe |
|---|---|---|---|---|---|---|---|---|---|---|---|---|
| **$CGRP_{(8-37)}$** | 3.08(3) | 2.86(3) | 4.16(4) | 1.03(1) | 2.01(2) | 1.94(2) | 2.02(2) | 1.09(1) | 4.88(5) | 1.86(2) | 3.00(3) | 1.98(2) |
| **bzl-$CGRP_{(8-37)}$** | 3.04(3) | 2.99(3) | 4.10(4) | 1.04(1) | 1.97(2) | 2.10(2) | 2.12(2) | 1.11(1) | 3.90(5) | 1.87(2) | 2.85(3) | 1.86(2) |
| **bzl-bn-$CGRP_{(8-37)}$** | 3.02(3) | 2.81(3) | 4.11(4) | 0.03(1) | 2.06(2) | 1.84(2) | 2.01(2) | 1.00(1) | 4.03(5) | 1.86(2) | 3.01(3) | 1.92(2) |

Theoretical values are shown in parentheses.

[a] Benzylation of His at position 10 results in loss of the histidyl residue in the composition.

[b] Benzoylation of the N-terminus results in low recovery due to incomplete hydrolysis of the N-α-benzoyl-$Val^8$ bond.

**Table 2.** Antagonist equilibrium dissociation constants ($K_B$ and $pA_2$) and Schild slopes for $CGRP_{(8-37)}$, bzl-$CGRP_{(8-37)}$ and bzl-bn-$CGRP_{(8-37)}$ in the mouse thoracic aorta and human SK-N-MC cells.

| | Mouse Thoracic Aorta[a] | | | Human SK-N-MC Cells[b] | | |
|---|---|---|---|---|---|---|
| | $K_B$ (nM) | $pA_2$ | Schild Slope | $K_B$ (nM) | $pA_2$ | Schild Slope |
| $CGRP_{(8-37)}$ | 1000.3 ± 0.19[d] | 6.4[d] | 0.8 ± 0.06 | 797.0 ± 0.38[d] | — | — |
| bzl-$CGRP_{(8-37)}$ | 88.9 ± 0.25[c] | 7.1[c] | 1.1 ± 0.27 | 15.4 ± 0.12[c] | — | — |
| bzl-bn-$CGRP_{(8-37)}$ | 22.9 ± 0.21[c] | 7.3[c] | 1.3 ± 0.01 | 0.65 ± 0.06[c,d,e] | 9.2[e] | 0.9 ± 0.14 |

[a] Each value is the mean ± S.E.M. of four to six experiments using separate aortas, each taken from different animals.

[b] Each value is the mean ± S.E.M. of three experiments performed in duplicate, each using different groups of cells,.

[c] Significantly different from $CGRP_{(8-37)}$ within a tissue or cell line ($p < 0.05$).

[d] Significantly different from bzl-$CGRP_{(8-37)}$ within a tissue or cell line ($p < 0.05$).

[e] Significantly different from the corresponding value in mouse thoracic aorta ($p < 0.05$).

JPET Fast Forward. Published on July 27, 2006 as DOI: 10.1124/jpet.106.108316


# Fig 1

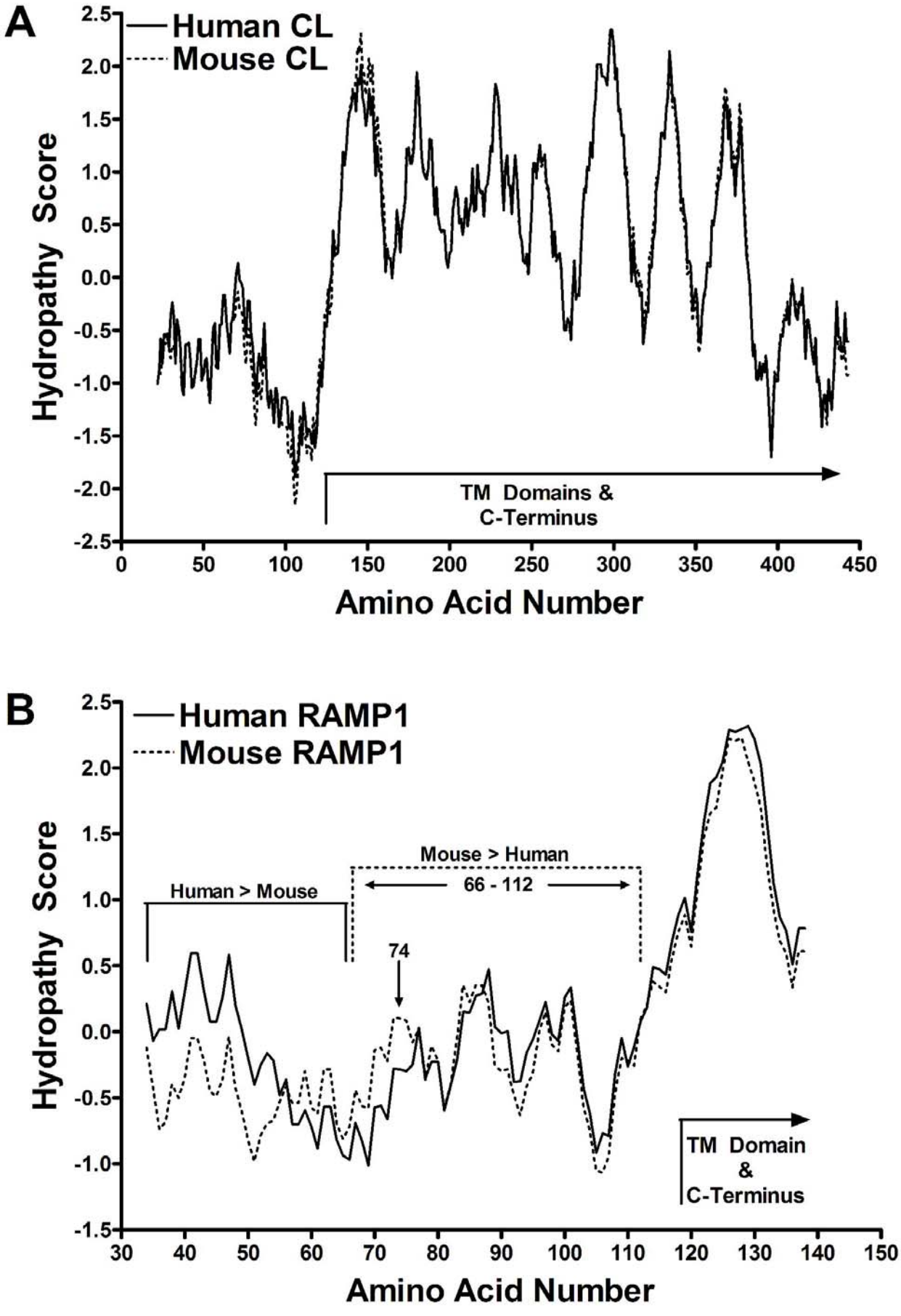

JPET Fast Forward. Published on July 27, 2006 as DOI: 10.1124/jpet.106.108316
This article has not been copyedited and formatted. The final version may differ from this version.

# Fig 2

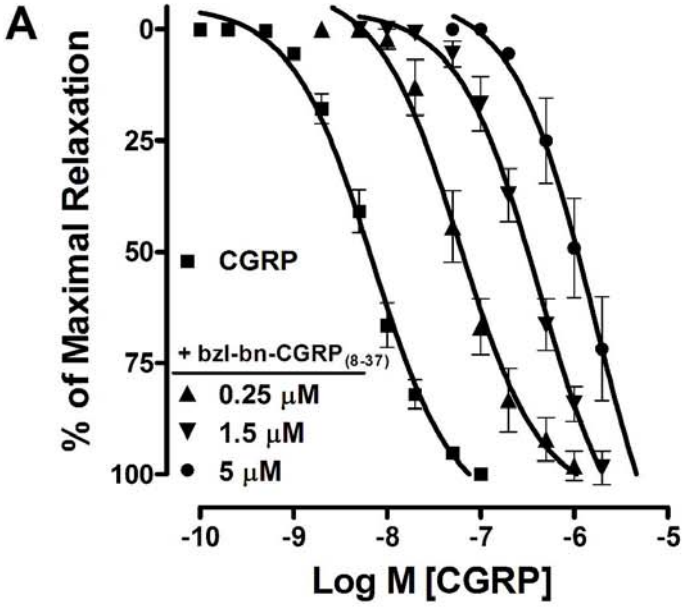


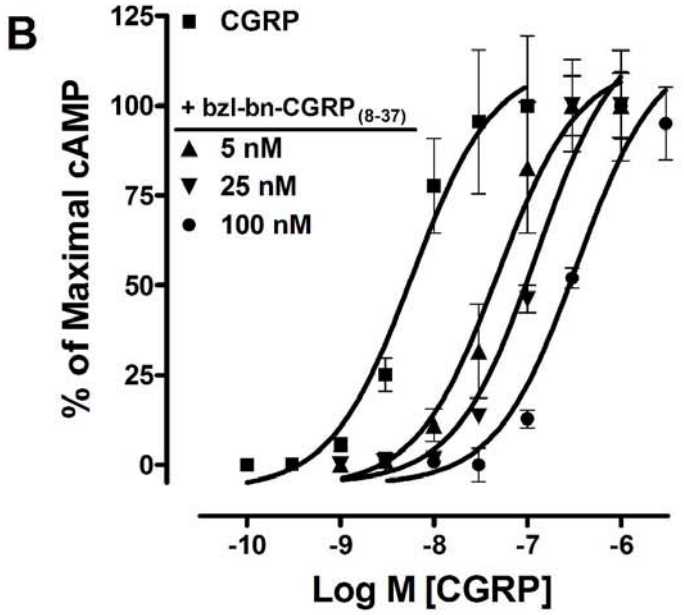


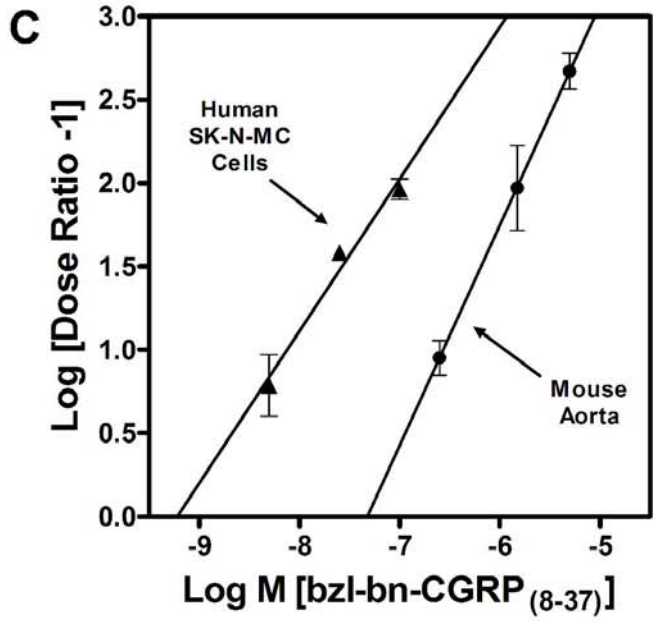

JPET Fast Forward. Published on July 27, 2006 as DOI: 10.1124/jpet.106.108316
This article has not been copyedited and formatted. The final version may differ from this version.

# Fig 3

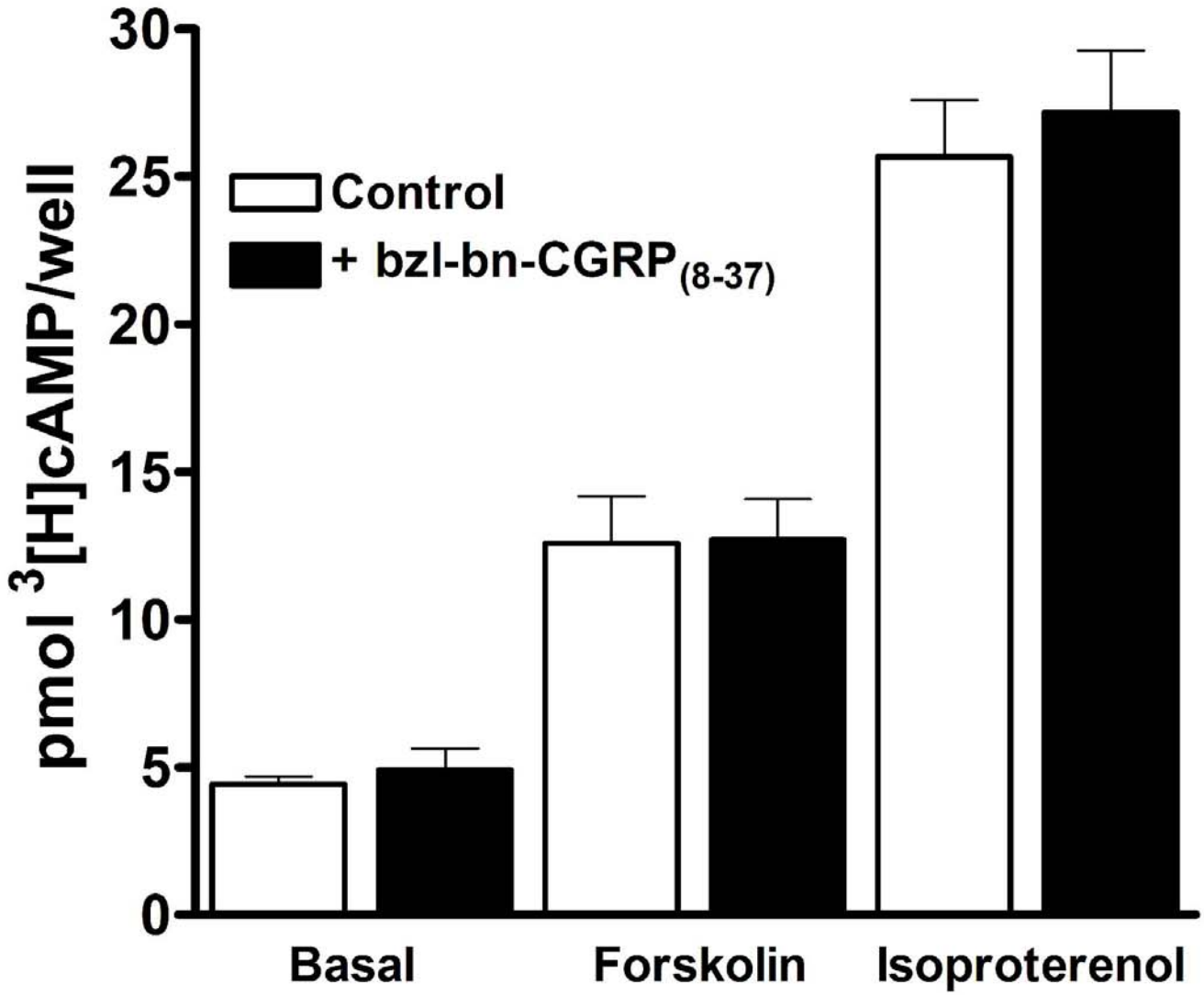

JPET Fast Forward. Published on July 27, 2006 as DOI: 10.1124/jpet.106.108316


# Fig 4